

# Ground-state energy and spin gap of spin- $\frac{1}{2}$ Kagomé-Heisenberg antiferromagnetic clusters: Large-scale exact diagonalization results

Andreas M. Läuchli,<sup>1,2,\*</sup> Julien Sudan,<sup>3</sup> and Erik S. Sørensen<sup>4,†</sup>

<sup>1</sup>Max-Planck-Institut für Physik komplexer Systeme, Nöthnitzer Str. 38, D-01187 Dresden, Germany

<sup>2</sup>Institut für Theoretische Physik, Universität Innsbruck, A-6020 Innsbruck, Austria

<sup>3</sup>Institut Romand de Recherche Numérique en Physique des Matériaux (IRRMA), CH-1015 Lausanne, Switzerland

<sup>4</sup>Department of Physics and Astronomy, McMaster University, Hamilton, Ontario L8S 4M1, Canada

(Received 8 March 2011; revised manuscript received 14 April 2011; published 3 June 2011)

We present a comprehensive list of the ground-state energies and the spin gaps of finite Kagomé clusters with up to 42 spins obtained using large-scale exact diagonalization techniques. This represents the current limit of this exact approach. For a fixed number of spins  $N$ , we study several cluster shapes under periodic boundary conditions in both directions resulting in a toroidal geometry. The clusters are characterized by their side length and diagonal as well as the shortest “Manhattan” diameter of the torii. A finite-size scaling analysis of the ground-state energy as well as the spin gap is then performed in terms of the shortest toroidal diameter as well as the shortest “Manhattan” diameter. The structure of the spin-spin correlations further supports the importance of short loops wrapping around the torii.

DOI: [10.1103/PhysRevB.83.212401](https://doi.org/10.1103/PhysRevB.83.212401)

PACS number(s): 75.10.Jm, 75.10.Kt, 75.40.Mg

The quest for magnetic materials and model systems exhibiting quantum spin liquid behavior is of considerable current experimental and theoretical interest. Among such systems, the Kagomé  $S = 1/2$  antiferromagnet stands out as a prototypical highly frustrated quantum magnet in two spatial dimensions<sup>1</sup> that potentially could exhibit spin liquid behavior. However, a complete understanding of this deceptively simple model given by

$$H = J \sum_{(i,j)} \mathbf{S}_i \cdot \mathbf{S}_j, \quad (1)$$

has proven surprisingly difficult and exact diagonalization (ED) results on this model, despite their limitation to very modest system sizes, have become crucial for both theoretical developments and nonexact numerical techniques.

Several ED simulations were carried out to explore puzzling facets of the Kagomé antiferromagnet.<sup>2–14</sup> ED established some of its remarkable properties, such as the absence of magnetic order and the enormously high number of singlet excitations below the lowest spinful excitation. Complementary computational techniques have also been applied to the Kagomé-Heisenberg antiferromagnet including series expansions,<sup>15–17</sup> quantum Monte Carlo,<sup>18</sup> diagonalizations in the nearest-neighbor valence bond basis and variants thereof,<sup>19–21</sup> contractor renormalization (CORE),<sup>22,23</sup> multi-scale entanglement renormalization ansatz (MERA),<sup>24</sup> and the density matrix renormalization group (DMRG).<sup>25,26</sup>

In this work, we report on large scale ED results for the ground-state energy and the spin gap of the Heisenberg  $S = 1/2$  antiferromagnet on various Kagomé samples consisting of up to  $N = 42$  spins. This considerable increase in system sizes (and Hilbert space size) was made possible by a distributed memory parallelization of our ED codes. We provide a finite size scaling of the ground-state energy and the spin gap as a function of the shortest diameter of the torii, which seems to capture the finite size dependence in a more systematic way than a simple  $1/N$  scaling used previously.<sup>7,8,14</sup>

## I. THE CLUSTERS

The list of the clusters used in this study along with their properties is given in Table I. For a given number of spins,  $N$ , we list several clusters in most of the cases. For a given  $N$ , there are many such clusters and the ones we list are chosen to be close to optimal, where optimal refers to a cluster that would have the length of both sides as well as the shortest diagonal all equal. This is considered optimal since such a cluster would be more likely to have the full point group symmetry of the infinite Kagomé lattice. Of the clusters, we consider only 12, 27b, and 36d to have the full symmetry of the Kagomé plane and they are therefore shown in bold. The basis vectors  $\mathbf{a}, \mathbf{b}$  of all clusters are given in terms of the vectors  $\mathbf{a}_1, \mathbf{a}_2$  shown in Fig. 1 where the two largest clusters 42a and 42b are shown. We also list the shortest *Manhattan diameter*,  $d_M$ , of each cluster. This measure can be visualized by tiling the plane with the cluster and finding the shortest path between two equivalent sites walking along the bonds of the lattice. Then,  $d_M$  is simply equal to the number of bonds traversed. We also define the shortest *geometrical diameter*, this is simply  $\text{Min}(|a|, |b|)$ . We also list the number of elements of the symmetry group,  $|G|$ , for nearest-neighbor interactions on the cluster. Note that clusters 18b, 21, 24, 27b have larger symmetry groups than expected based on the applicable symmetries of the infinite Kagomé lattice.

## II. ED ON DISTRIBUTED SYSTEMS

Typically, an ED study of a cluster would involve a complete symmetry analysis of the cluster and resulting spectra. Then, one could write the Hamiltonian matrix restricted to a given symmetry sector to a file that would be read into memory for diagonalization. Using *shared memory* systems, this has been achieved in the past for a specific quantum number sector for 42 spins on the star lattice.<sup>27</sup> However, this approach becomes impossible for the larger system sizes and symmetry sectors included in this study, because writing or storing the Hamiltonian becomes prohibitively slow and matrix elements

TABLE I. Cluster studied in this work. Listed are the number of spins  $N$ ; the basis vectors  $\mathbf{a}, \mathbf{b}$  in terms of  $\mathbf{a}_1$  and  $\mathbf{a}_2$  (each of length  $2a$ ); the length of the basis vectors,  $(|\mathbf{a}|, |\mathbf{b}|)$ , in units of  $2a$  along with the length of the diagonal  $d = \min(|\mathbf{a} - \mathbf{b}|, |\mathbf{a} + \mathbf{b}|)$ ; the Manhattan length,  $d_M$ , the length of the shortest loop wrapping around the torus; the number of elements of the symmetry group  $|G|$ ; the total ground-state energy,  $E$ ; the energy per site,  $E/N$ ; and the value of the spin gap,  $\Delta$ , between the  $S = 0$  ground state and the lowest  $S = 1$  state for even samples or the gap from the  $S = 1/2$  ground state to the lowest  $S = 3/2$  state for odd samples. Results shown in bold are for clusters with the full symmetry of the Kagomé plane.

$N$	$\mathbf{a}, \mathbf{b}$	$ \mathbf{a} $	$ \mathbf{b} $	$d$	$d_M$	$ G $	Total $E$ (J)	$E/N$	$\Delta$
<b>12</b>	<b>(2,0), (0,2)</b>	<b>2</b>	<b>2</b>	<b>2</b>	<b>4</b>	<b>48</b>	<b>-5.444 875 216</b>	<b>-0.453 740</b>	<b>0.382 668 366</b>
15	(2,-1), (-1,3)	$\sqrt{3}$	$\sqrt{7}$	$\sqrt{7}$	4	20	-6.589 143 829	-0.439 276	0.418 800 403
18 a	(2,-1), (0,3)	$\sqrt{3}$	3	$\sqrt{12}$	4	24	-8.064 482 605	-0.448 027	0.270 115 263
18 b	(2,-2), (-2,-1)	2	$\sqrt{7}$	3	4	48	-8.048 270 773	-0.447 126	0.284 567 177
21	(2,1), (-1,3)	$\sqrt{7}$	$\sqrt{7}$	$\sqrt{7}$	6	336	-9.172 279 619	-0.436 775	0.278 637 026
24	(1,2), (-3,2)	$\sqrt{7}$	$\sqrt{7}$	$\sqrt{12}$	6	96	-10.589 965 547	-0.441 249	0.207 828 742
27 a	(2,1), (-3,3)	$\sqrt{7}$	3	$\sqrt{13}$	6	18	-11.793 996 213	-0.436 815	0.275 413 255
<b>27 b</b>	<b>(3,0), (0,3)</b>	<b>3</b>	<b>3</b>	<b>3</b>	<b>6</b>	<b>216</b>	<b>-11.779 504 985</b>	<b>-0.436 278</b>	<b>0.268 776 803</b>
30	(2,1), (-2,4)	$\sqrt{7}$	$\sqrt{12}$	$\sqrt{13}$	6	20	-13.154 318 948	-0.438 477	0.152 855 536
33	(1,2), (4,-3)	$\sqrt{7}$	$\sqrt{13}$	$\sqrt{19}$	6	22	-14.410 195 048	-0.436 673	0.229 455 039
36 a	(-2,3), (4,0)	$\sqrt{7}$	4	$\sqrt{19}$	6	24	-15.787 874 847	-0.438 552	0.144 945 554
36 b	(3,0), (-3,4)	3	$\sqrt{12}$	$\sqrt{21}$	6	48	-15.806 927 756	-0.439 081	0.170 275 671
36 c	(3,0), (-1,4)	3	$\sqrt{13}$	4	6	24	-15.814 334 002	-0.439 287	0.184 874 846
<b>36 d</b>	<b>(4,-2), (-2,4)</b>	<b><math>\sqrt{12}</math></b>	<b><math>\sqrt{12}</math></b>	<b><math>\sqrt{12}</math></b>	<b>8</b>	<b>144</b>	<b>-15.781 555 119</b>	<b>-0.438 377</b>	<b>0.164 189 901</b>
39 a	(-1,3), (5,-2)	$\sqrt{7}$	$\sqrt{19}$	$\sqrt{21}$	6	26	-17.038 187 797	-0.436 877	0.199 163 545
39 b	(1,3), (-3,4)	$\sqrt{13}$	$\sqrt{13}$	$\sqrt{13}$	8	78	-17.020 192 866	-0.436 415	0.222 433 924
42 a	(-1,3), (5,-1)	$\sqrt{7}$	$\sqrt{21}$	$\sqrt{28}$	6	28	-18.395 959 984	-0.437 999	0.120 425
42 b	(-2,4), (4,-1)	$\sqrt{12}$	$\sqrt{13}$	$\sqrt{19}$	8	28	-18.401 988 921	-0.438 143	0.149 092 139

have to be calculated on-the-fly. Furthermore, the largest sectors do not fit into accessible shared memory machines anymore, such that these large system sizes are *only* treatable on *distributed memory* systems where each computational node only has a relatively small addressable memory space, typically a few giga bytes (or less). In general, it is much easier and cheaper to scale a distributed system to a large combined memory space than a shared memory system and

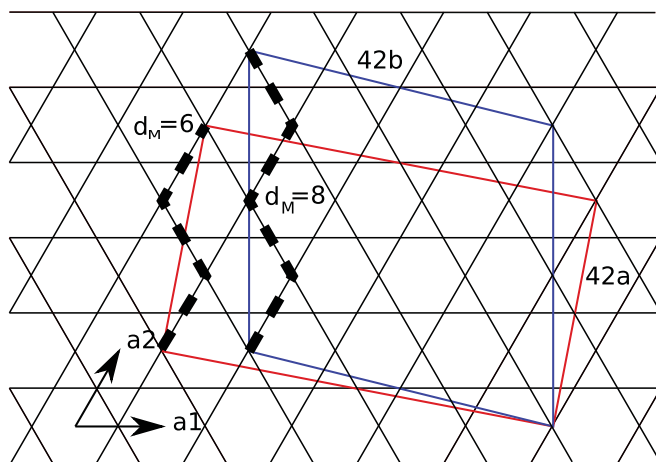


FIG. 1. (Color online) The two 42-site Kagomé clusters used in this study. The shortest Manhattan diameters,  $d_M$ , are shown as thick dashed lines.

future large ED studies will likely have to be performed on distributed systems. Due to the physical constraints of a distributed memory system some peculiarities remain: A Lanczos diagonalization proceeds by iteratively performing,  $N_{it}$ , matrix vector multiplications on vectors of length,  $M$ . If treating one element of the vector requires a time  $t$ , the full cpu time for the calculation is roughly,  $N_{it}Mt$ . Due to the memory constraints of distributed systems the application of a nontrivial symmetry that would reduce  $M$  by a factor of  $K$  almost always will increase  $t$  by a factor *larger* than  $K$ , even when the number of cpu's used is the same. The result is that it is *slower* to diagonalize the smaller symmetry reduced Hamiltonian than the full one. For the largest clusters we therefore only use very few simple symmetries. For the 42-site clusters when no lattice symmetries were used the resulting maximal Hilbert space dimension is then  $\binom{42}{21}/2 = 269'128'937'220$ .

### III. RESULTS

Our main result is Table I listing the ground-state energy and the spin gap of the samples considered in this work. Some of the smaller samples have already been studied in the past and energies were quoted for 12, 15, 18b, and 21 in Refs. 3 and 5<sup>28</sup> for 27b in Refs. 5 and 7 and for 36d in Refs. 5 and 8. An approximate ground-state energy and spin gap of the sample 36c have been obtained by DMRG in Ref. 25.

We plot the ground-state energies as a function of the inverse geometrical diameter, which in our convention corresponds to  $1/|\mathbf{a}|$  and display the result in Fig. 2. This presentation seems

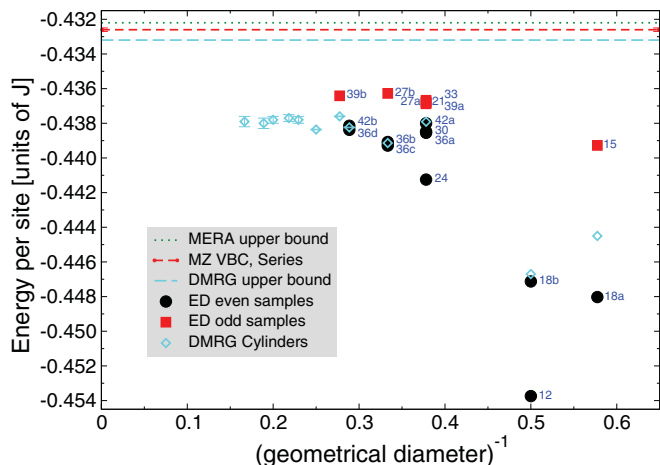


FIG. 2. (Color online) Ground-state energy per site plotted as a function of the inverse shortest geometrical diameter. Remarkably good agreement with recent DMRG results<sup>26</sup> on long cylinders with the same diameter is observed. For comparison, we also display the MERA upper bound,<sup>24</sup> series expansion results for the Marston-Zeng valence bond crystal,<sup>16,17</sup> as well as the DMRG upper bound.<sup>26</sup>

to capture the finite size effects in a more systematic way than the previously used  $1/N$  scaling, as the data seem to behave consistently upon increasing the system size, while keeping the diameter constant. Furthermore, we observe good agreement with recent DMRG data<sup>26</sup> on long cylinders with the same diameter, thus corroborating the accuracy of the DMRG simulations.

Next, we plot the spin gap data in Fig. 3 in the same way. For each diameter, we observe that the spin gap is monotonously decreasing with system size (for even and odd samples separately). While it is difficult to extrapolate the ED spin gap for constant diameter due to a lack of system sizes for large diameters, the qualitative agreement with DMRG results on long cylinders suggests that it is indeed the diameter which controls the finite size effects upon moving toward the two-dimensional bulk limit.

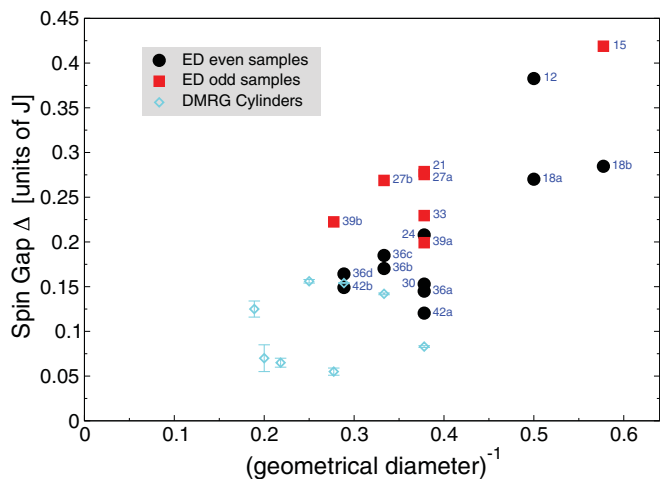


FIG. 3. (Color online) Spin gap of even and odd Kagomé samples obtained by ED and plotted as a function of the inverse shortest geometrical diameter. For comparison, recent DMRG data<sup>26</sup> obtained on long cylinders with the same diameter are shown.

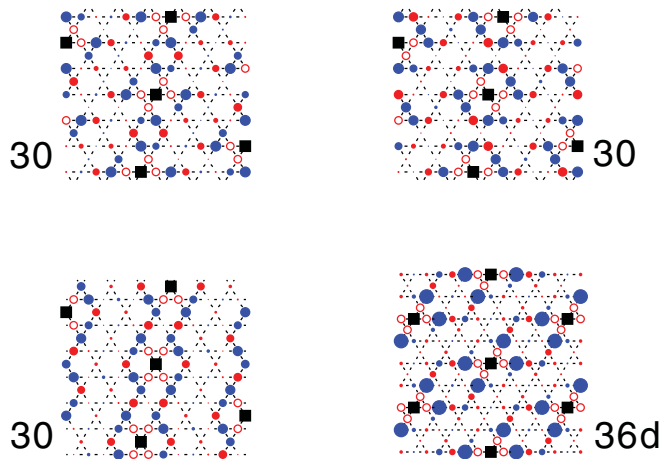


FIG. 4. (Color online) Magnified spin-spin correlations in the ground state of the 30 and 36d Kagomé samples. The 30-site cluster with its low symmetry requires three distinct reference sites to be considered. The diameter of the circle is proportional to the magnitude of the spin-spin correlation with the reference site (black filled square). Dark blue (light red) color denotes positive (negative) correlations. The nearest-neighbor correlations (all antiferromagnetic) have been dropped for clarity. One observes pronounced staggered spin-spin correlations along selected loops wrapping around the torus in the left two panels and the lower right panel.

Complementary evidence for the important role played by short loops wrapping around the torus is provided by a magnified view on the spin-spin correlations in the ground state of several even samples displayed in Fig. 4 (see Ref. 5 for tabulated values of sample 36d). In a spin liquid with a very short correlation length, one would expect spin correlations between distant sites to be very weak and also not to depend significantly on the sample geometry. Indeed, in Fig. 4, most spin-spin correlations are quite weak, but pronounced staggered spin-spin correlations along selected loops wrapping around the sample are revealed. We expect these resonances to disappear once the samples are sufficiently wide.

#### IV. CONCLUSIONS

We have presented a systematic study of the ground-state energies and the spin gaps of many Kagomé clusters. In particular, we have presented results for  $N = 39, 42$  obtained on distributed memory parallel clusters. Future quantum numbered resolved ED studies on the largest samples should allow to check the appearance of the topological degeneracy required for the  $\mathbb{Z}_2$  spin liquid advocated in Ref. 26.

#### ACKNOWLEDGMENTS

We thank D. A. Huse for useful correspondence on sample geometries and are grateful to D. A. Huse, R. Moessner, and S. R. White for discussions. A.M.L. acknowledges support by the MPG RZG and allocation of computing time on the PKS-AIMS and the BlueGene/P machines at the MPG RZG. E.S.S. acknowledges allocation of computing time at the Shared Hierarchical Academic Research Computing Network (SHARCNET:www.sharcnet.ca) and support by NSERC.

\*aml@pks.mpg.de

†sorensen@mcmaster.ca

- <sup>1</sup>L. Balents, *Nature* **464**, 199 (2010).
- <sup>2</sup>V. Elser, *Phys. Rev. Lett.* **62**, 2405 (1989).
- <sup>3</sup>C. Zeng and V. Elser, *Phys. Rev. B* **42**, 8436 (1990).
- <sup>4</sup>J. T. Chalker and J. F. G. Eastmond, *Phys. Rev. B* **46**, 14201 (1992).
- <sup>5</sup>P. W. Leung and V. Elser, *Phys. Rev. B* **47**, 5459 (1993).
- <sup>6</sup>N. Elstner and A. P. Young, *Phys. Rev. B* **50**, 6871 (1994).
- <sup>7</sup>P. Lecheminant, B. Bernu, C. Lhuillier, L. Pierre, and P. Sindzingre, *Phys. Rev. B* **56**, 2521 (1997).
- <sup>8</sup>C. Waldtmann, H.-U. Everts, B. Bernu, C. Lhuillier, P. Sindzingre, P. Lecheminant, and L. Pierre, *Eur. Phys. J. B* **2**, 501 (1998).
- <sup>9</sup>P. Sindzingre, G. Misguich, C. Lhuillier, B. Bernu, L. Pierre, Ch. Waldtmann, and H.-U. Everts, *Phys. Rev. Lett.* **84**, 2953 (2000).
- <sup>10</sup>Ch. Waldtmann, H. Kreutzmann, U. Schollwöck, K. Maisinger, and H.-U. Everts, *Phys. Rev. B* **62**, 9472 (2000).
- <sup>11</sup>J. Richter, J. Schulenburg, and A. Honecker, *Lect. Notes Phys.* **645**, 85 (2004).
- <sup>12</sup>A. Läuchli and C. Lhuillier, Dynamical correlations of the Kagome  $S = 1/2$  Heisenberg quantum antiferromagnet, e-print [arXiv:0901.1065](https://arxiv.org/abs/0901.1065).
- <sup>13</sup>E. S. Sørensen, M. J. Lawler, and Y. B. Kim, *Phys. Rev. B* **79**, 174403 (2009).
- <sup>14</sup>P. Sindzingre and C. Lhuillier, *Europhys. Lett.* **88**, 27009 (2009).
- <sup>15</sup>R. R. P. Singh and D. A. Huse, *Phys. Rev. Lett.* **68**, 1766 (1992).
- <sup>16</sup>R. R. P. Singh and D. A. Huse, *Phys. Rev. B* **76**, 180407(R) (2007).
- <sup>17</sup>R. R. P. Singh and D. A. Huse, *Phys. Rev. B* **77**, 144415 (2008).
- <sup>18</sup>M. Nyfeler, F.-J. Jiang, F. Kämpfer, and U.-J. Wiese, *Phys. Rev. Lett.* **100**, 247206 (2008).
- <sup>19</sup>C. Zeng and V. Elser, *Phys. Rev. B* **51**, 8318 (1995).
- <sup>20</sup>M. Mambrini and F. Mila, *Eur. Phys. J. B* **17**, 651 (2000).
- <sup>21</sup>D. Poilblanc, M. Mambrini, and D. Schwandt, *Phys. Rev. B* **81**, 180402 (2010).
- <sup>22</sup>R. Budnik and A. Auerbach, *Phys. Rev. Lett.* **93**, 187205 (2004).
- <sup>23</sup>S. Capponi, A. Läuchli, and M. Mambrini, *Phys. Rev. B* **70**, 104424 (2004).
- <sup>24</sup>G. Evenbly and G. Vidal, *Phys. Rev. Lett.* **104**, 187203 (2010).
- <sup>25</sup>H. C. Jiang, Z. Y. Weng, and D. N. Sheng, *Phys. Rev. Lett.* **101**, 117203 (2008).
- <sup>26</sup>S. Yan, D. A. Huse, and S. R. White, *Science* doi:10.1126/science.1201080.
- <sup>27</sup>J. Richter, J. Schulenburg, A. Honecker, and D. Schmalfuß, *Phys. Rev. B* **70**, 174454 (2004).
- <sup>28</sup>The spin gap for 15, the energy and spin gap for 18b, and the spin gap for 21 seem to be incorrect in Ref. 3, see Ref. 5 and our results.